Aldehyde-Amine Chemistry Enables Modulated Biosealants with Tissue-Specific Adhesion

By *Natalie Artzi, Tarek Shazly, Aaron B. Baker, Adriana Bon,* and *Elazer R. Edelman**

Soft-tissue surgical sealants provide an ideal material class for assessment of tissue–material interactions. Sealant adhesion can be rigorously quantified through a series of functional assays that supplement characterizations of tissue reactivity and material fate. A collection of experimental techniques can be exploited to elucidate mechanistic aspects of tissue–material interactions with general implications, extending beyond the immediate scope of adhesive materials. Moreover, though sealants are routinely used in clinical procedures, active questions and limitations force physicians to choose between extremes of adhesion strength and biocompatibility.[1] Common cyanoacrylate derivatives adhere strongly to tissue, but their vigorous and uncontrolled tissue crosslinking along with the release of toxic degradation by-products dramatically impedes healing and regeneration processes.[2] The polymerization of alkylcyanoacrylates occurs via anionic and zwitterionic polymerizations in the presence of weak bases such as alcohols, water, and amino acids encountered in living tissues.[3] Cyanoacrylates with short side alkyl chains (methyl or ethyl) rapidly degrade to form cyanoacetate and formaldehyde, characterized by acute and chronic inflammation. The longer alkyl chains degrade slower, resulting in more limited accumulation of toxic byproducts that may be effectively eliminated by tissues. Histotoxicity depends on the vascularity of tissues, being greater in well-vascularized soft tissues.[4] Fibrin glues represent the opposite polar extreme along the spectrum of sealants[4] eliciting a mild tissue response, but with relatively non-specific and minimally adhesive tissue interaction.[5–7] Though these and all sealants rely on intimate tissue–material interactions for functional adhesion, target-tissue properties have been largely ignored in material design. Instead, one general formulation is proposed for application to the full range of soft tissues across diverse clinical applications.[8–13] Here, we demonstrate that aldehyde-mediated adhesion to tissue strongly depends on target-tissue type and state, and propose a rational approach for the engineering of application-specific surgical sealants.

Copolymeric hydrogels featuring aminated star polyethylene glycol and high-molecular-weight dextran aldehyde (PEG:dextran) possess a series of physico-chemical properties that can be modified to create a family of materials with tunable tissue adhesion.[14–17] The two polymer constituents of PEG:dextran were prepared as minimally viscous aqueous solutions and consistently polymerized through injection from a dual chamber syringe equipped with a mixing tip.[15,16] The cohesive integrity of PEG:dextran is derived from imine bonds that form through a Schiff base reaction between amines and aldehydes.[14–17] When crosslinked on soft-tissue surfaces, aldehydes not consumed in bulk network formation form analogous bonds with tissue amines to achieve adhesion. Aldehydes in excess of what is required for cohesion or adhesion can induce tissue toxicity.[18] Consequently, material aldehyde density is the key design parameter for informative evaluation of tissue-material adhesion and tissue response. We designed and evaluated a series of PEG:dextran formulations featuring low (8.8%, abbreviated L-PD), medium (14.0%, abbreviated M-PD), and high (20.0%, abbreviated H-PD) levels of dextran aldehyde solid content. Additional design parameters, including dextran molecular weight (10 kDa) and oxidation state (50%), and PEG amine solid content (25%) were identical among formulations, and selected to provide stable and bioreactive networks for evaluation of adhesive interactions.[17]

Here, we demonstrate that PEG:dextran adhesion is tissue-specific, and can be readily adjusted through manipulation of material aldehyde content. Because adhesion is mediated through material crosslinking to local tissue amines, judicious modification of formulation aldehyde content is a logical approach to ensure sufficient adhesion strength for a given clinical scenario. However, biochemical variations among soft tissues in various states forces one to consider the aldehyde affinity of target tissue in compositional design. The need for careful titration of material composition is reiterated by the in vivo tissue response to PEG:dextran, as local inflammation and general tissue toxicity are also related to material aldehyde density. These concepts define a therapeutic window for optimal tissue–sealant interactions, bounded below by the need for adequate adhesion strength and above by the condition of biocompatibility.

Adhesive mechanics were measured ex vivo with soft tissues harvested from rats immediately after animal sacrifice. Adhesive-test elements were constructed with biopsy specimens of uniform thickness (1 mm) from heart, lung, liver, and duodenal tissues to facilitate uniaxial mechanical testing of tissue–material interfaces (Fig. 1). The stress response of

[*] Prof. E. R. Edelman, Dr. N. Artzi, T. Shazly, Dr. A. B. Baker
Harvard-MIT Division of Health Sciences and Technology
Massachusetts Institute of Technology
Cambridge, Massachusetts 02139 (USA)
Cardiovascular Division, Department of Medicine
Brigham and Women's Hospital
Harvard Medical School
Boston, Massachusetts 02115 (USA)
E-mail: ere@mit.edu
A. Bon
Institut Quimic de Sarria'
Universitat Ramon Llull
Barcelona 08017 (Spain)

DOI: 10.1002/adma.200900340

© 2009 WILEY-VCH Verlag GmbH & Co. KGaA, Weinheim

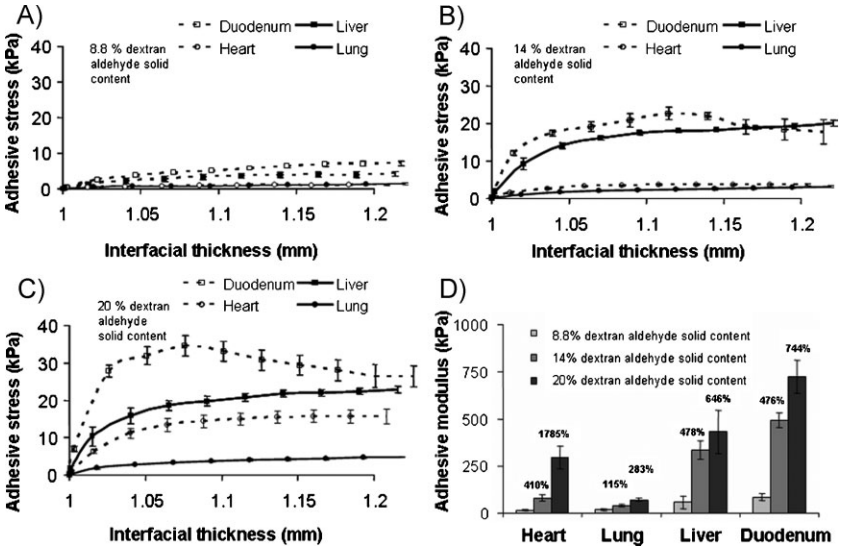

Figure 1. The adhesion of PEG:dextran-based adhesives depends on tissue type (heart, lung, liver, or duodenal rat biopsies) and constituent chemistry, evaluated at low [A) 8.8 wt%], medium [B) 14.0 wt%], or high [C) 20.0 wt%] concentrations of dextran aldehyde solid content. The moduli of the adhesive test elements increased with aldehyde content dependant on tissue type D). The increase in modulus compared to low aldehyde content is presented above the bars for medium and high content variants.

adhesive test elements over a range of applied displacement varied with material aldehyde content and tissue type (Fig. 1A–C). The interfacial modulus was calculated from the initial stress response ($1 <$ interfacial thickness < 1.05) and serves as a convenient metric for comparison of adhesive mechanics. Adhesive stiffness varied dramatically in response to material chemistry and tissue type (Fig. 1D). The modulus of H-PD adhesion to duodenal test elements (724 ± 86 kPa) was significantly greater ($p < 0.001$) than lung (72 ± 7 kPa), while heart and liver moduli were comparatively intermediate (296 ± 60, 431 ± 15 kPa, respectively). The extent to which aldehyde content altered stiffness at tissue interfaces is tissue-specific. Cardiac tissue-test elements exhibited the greatest relative increase in interfacial stiffness when comparing L-PD and H-PD variants (1785%), while lung tissue had a much weaker dependence (283%). Overall, these data support the notion that both tissue type and material chemistry influence aldehyde-mediated adhesive interactions, providing a functional basis for tissue-specific sealant design.

The tissue response to subcutaneous material implants was used to evaluate the in vivo biocompatibility of PEG:dextran materials and particularly the influence of material aldehyde content on tissue response. PEG:dextran variants (L-PD, M-PD, and H-PD) were implanted into a subcutaneous pocket in mice that survived for nine days. Inflammation as manifested by thicker fibrous capsule increased with aldehyde content (Fig. 2A). Inflammatory cell-mediated proteolysis affects wound repair as matrix metalloproteases cleave the extracellular matrix weakening the tissue and surgical anastomoses.[19] The gelatinase activity in the tissues, measured using analytical fluorescent microscopy and in situ zymography, also increased with material aldehyde content (Fig. 2B). This trend in proteolytic activity is likely a result of the increased pro-inflammatory mediators and activation of polymorphonuclear leukocytes generated by the reactive aldehyde groups.

The conjugation of aldehyde-coated fluorescent microspheres (f-MS) to soft tissues was used to probe tissue-surface chemistry and provide a mechanistic basis for the demonstrated variability in adhesive mechanics. Tissue biopsies of controlled surface area were excised from rat heart, lung, liver, and duodenum and allowed to react with f-MS through gentle mixing in an aqueous solution. Following suspension, the fluorescent intensity at the surface of the tissue samples was quantified to generate an aldehyde conjugation metric reflecting the percent of tissue-surface coverage by immobilized f-MS (Fig. 3A). The conjugation metric is indicative of the aldehyde affinity of soft tissues, and provides a fairly direct measure of the targeted biochemistry for PEG:dextran adhesion. Soft tissues display a range of f-MS conjugation metrics, with duodenal tissue possessing the greatest apparent aldehyde affinity. Comparison of tissue-conjugation metrics to adhesive mechanical data provides convincing evidence for aldehyde-mediated adhesion, as interfacial moduli strongly correlate ($R = 0.92$, $p < 0.05$)

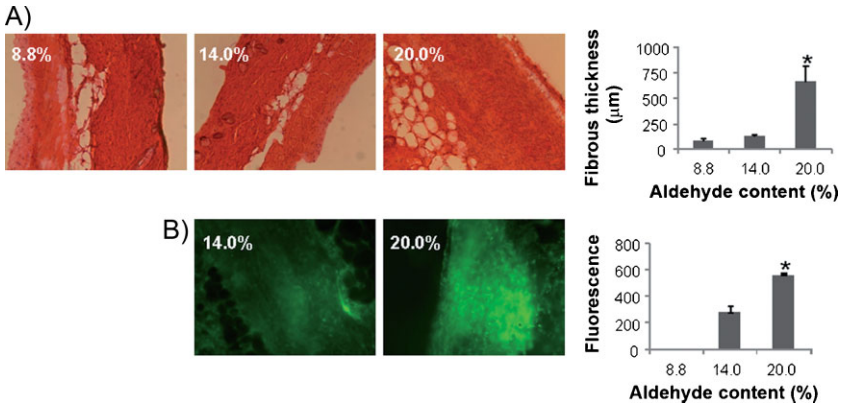

Figure 2. Tissue reactivity in vivo was assessed for subcutaneous implants of materials having low (8.8 wt%), medium (14.0 wt%), or high (20.0 wt%) dextran aldehyde solid content. A subcutaneous pocket was created in anesthetized C57BL/6 mice and 200 μL of material was injected into the pocket using a syringe with mixing tip. After nine days, the mice were sacrificed and the skin and subcutaneous tissue were harvested. The samples were snap frozen in liquid nitrogen and stored at −80 °C until histological and zymographic analysis. Materials with increased aldehyde content cause an increased inflammatory response. A) Histomorphometric analysis reveals increased fibrotic capsule thickness and inflammatory cell present in materials with high aldehyde content. B) Gelatinase zymographic activity was increased with material aldehyde levels. (* $p < 0.05$ compared with 14.0% solid content).

WILEY InterScience DISCOVER SOMETHING GREAT
© 2009 WILEY-VCH Verlag GmbH & Co. KGaA, Weinheim

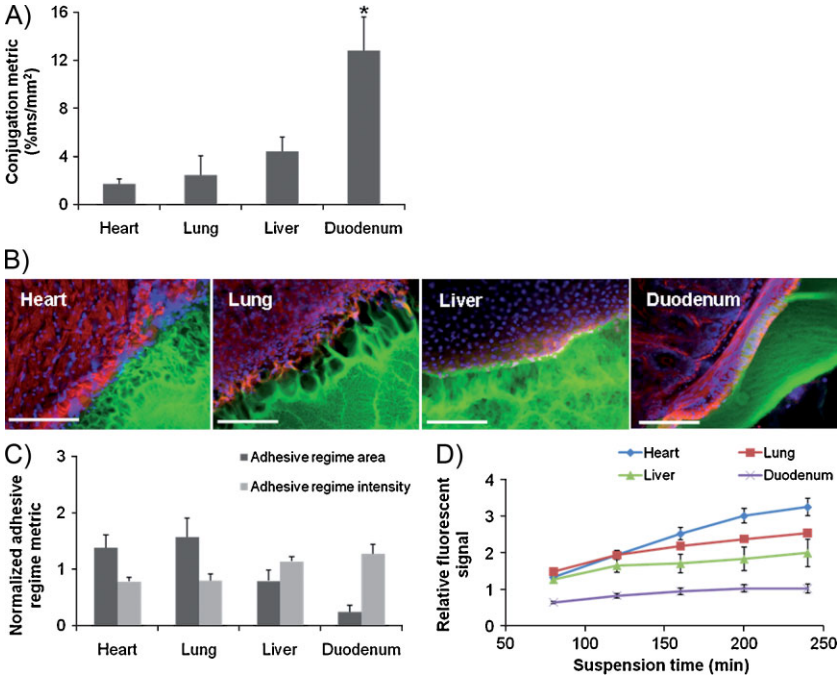

Figure 3. A) The relative aldehyde reactivity of heart, lung, liver, and duodenal rat tissue were assessed though tissue-sample conjugation of fluorescent aldehyde-coated microspheres. Aldehyde reactivity was lowest in the lung and heart, greater in the liver and highest in the duodenum (* $p < 0.05$ compared with liver and duodenum). B) The interface between PEG:dextran (green) and various soft tissues, highlighted with rhodamine phalloidin (actin, red) and DAPI (cell nuclei, blue), varies with tissue. C) Both the adhesive regime area (size normalized to interfacial length) and density (fluorescence intensity) demonstrate that tissues with high aldehyde reactivity form smaller and more continuous interfaces with PEG:dextran. * $p < 0.05$ compared with liver and duodenum. D) Differential adhesive retention was seen when applied to different tissues. Adhesive is most stable when applied to the duodenum while those applied to the liver, lung, and heart degrade faster and at an increasing rate. Degradation rate correlates with material affinity to the tissues ($R = 0.9$, $p < 0.05$).

to aldehyde affinity across the tested tissue types and material variants. The aldehyde content of materials and aldehyde affinity of tissue seemingly present a mechanism by which to design and select materials based on clinical applications.

The interfacial regions between PEG:dextran and excised rat heart, lung, liver, and duodenum tissues were microscopically examined to add physical insight to adhesive interactions. Three distinct domains were evident upon material adherence, including the target tissue, bulk material, and an adhesive regime interposed between the two (Fig. 3B). The adhesive regime depicts the intermediate material structure resulting from concurrent dextran aldehyde reactivity with PEG and tissue amines. The morphology of the adhesive regime varied with tissue, and reflected the strength of adhesion, appearing fibrillar and discontinuous on cardiac and lung tissues, and more continuous and intact over liver and duodenum. Quantitative microscopic evaluation of the adhesive regimes based on fluorescent material intensity provides normalized metrics of area per unit interfacial length (adhesive regime size) and the average material concentration (adhesive regime density). Significant differences in the resultant PEG:dextran morphology were measured following tissue-material adhesion (Fig. 3C). While the adhesive regime above duodenal tissue was minimal in size (0.24 ± 0.11) and comparatively dense (1.27 ± 0.17), interactions with heart, lung, and liver yielded more expansive and dispersed adhesive interfaces. Comparisons between adhesive morphology and mechanics confirmed common physical intuition, as both adhesive regime metrics strongly correlate to interfacial moduli ($R = 0.95$, $p < 0.05$, L-PD variant) across tissue types, indicating that small and dense material transitions between tissue and bulk yield stiff adhesive interactions.

The extent of tissue–material interaction should largely determine the tissue retention of an adhesive material. Fluorescent PEG:dextran materials were applied to tissue biopsies and submerged in media under defined conditions. The presence of released fluorescent signal was monitored as the media was periodically changed. This signal is a surrogate for the effective material loss from a tissue surface and varied based on underlying tissue type. Relatively rapidly fluorescent accumulation occurred when PEG:dextran was applied to heart and lung tissue, while hepatic and duodenal specimens exhibited protracted release kinetics (Fig. 3D). PEG amine content lost to the media evidentially depends on the material continuity at the tissue surface, as significant correlations of cumulative material loss to adhesive regime size and intensity ($R > 0.90$, $p < 0.05$) were found across tissue types.

Adhesive materials reside not only in normal, stable environments but in extremes of pH, oxygen content, and enzymatic challenge.[20,21] Small intestinal tissue pH, for example, rises from 5.9 to 6.2 in patients with Crohn's disease and to 6.6 for coeliac patients.[22] Imine bond formation is pH sensitive, suggesting that such variations in tissue state may affect aldehyde-mediated adhesion.[23] These bonds form when amines attack the aldehydes to form an intermediate product, and are then dehydrated to imine bonds. The first reaction is slow at acidic pH values, where a significant amount of amines are protonated. In contrast, the dehydration step is retarded at basic pH values, where protonation of the OH-leaving group is compromised. Hence, imine-bond formation is fastest near neutrality, which is well reflected in the pH sensitivity of PEG:dextran adhesive mechanics with treated duodenal tissue. Ultimate adhesive strength was highest at pH 7.4, and falls by 60% at pH 6 and 77% at pH 9. The moduli of the adhesive construct depict the same trend as that of ultimate adhesive strength; highest at pH 7.4, and 45 and 81% lower for pH 6 and 9.

Aldehyde-presenting PEG:dextran materials exhibit tissue- and pH-dependent adhesive properties. However, the benefit of increased adhesion of materials with greater aldehyde content must be balanced by adverse biologic responses to excess free aldehydes. Substantial differences in soft-tissue aldehyde affinity shift the balance between adhesion and inflammation for each

© 2009 WILEY-VCH Verlag GmbH & Co. KGaA, Weinheim

WILEY InterScience® DISCOVER SOMETHING GREAT

tissue, and suggests that a class of materials could be optimized for specific needs. Excess aldehydes might simply be minimized when tissues are less responsive to changes in material aldehyde content, as in the case of lung tissue. In the other tissues, where aldehyde affinity is higher and resultant adhesion more dynamic, the intense response to material chemistry allows one to consider designing compositions for anticipated duration and desired strength of adhesion. Though tissue-surface chemistry is often ignored, it is a critical determinant of tissue–material interaction. Unlike cyanoacrylate and fibrin glue, PEG:dextran-based materials have flexible design parameters that enable their mediation for specific applications. Quantification and consideration of tissue properties must be a part in the design of any adhesive material to advance material selection for the full range of target tissues and clinical needs. The performance of existing and future adhesive materials should be examined with regard to tissue specificity.

Experimental

PEG:Dextran: The synthesis of star PEG amine and dextran aldehydes as well as the PEG:dextran network formation have been previously described [14–17]. Briefly, eight-arm 10 kDa star PEG polymer with amine end groups was dissolved in water to form a 25 wt% aqueous solution. Linear dextran (10 kDa) was oxidized with sodium periodate to yield dextran aldehyde, which was also prepared as an aqueous solution (8.8–20.0 wt%). The present study examines the effect of aldehyde content on adhesion strength and tissue response, motivating the design and synthesis of a series of materials with isolated variation in dextran aldehyde solid content.

Fluorescent PEG Amine: To characterize the PEG:dextran morphology at the tissue–material interface as well as track gradual material release from the tissue surface, constituent PEG amine was labeled with fluorescein. PEG amine (2.4 g) was dissolved in 6 mL dichloromethane, followed by the addition of 0.015 g 6-(fluorescein-5-carboxyamido) hexanoic acid (Invitrogen) and 12 μL triethylamine (Sigma). The mixture was stirred at room temperature for 48 h. The resulting solid after solvent evaporation was dissolved in 100 mL water, dialyzed, and lyophilized. PEG amine solutions of 25 wt% solid content, 0.5% of which were fluorescently labeled, were then prepared and crosslinked with dextran aldehyde solutions in the established manner yielding fluorescent materials.

Subcutaneous Mouse Model: A subcutaneous implantation model of tissue response was used to evaluate in vivo compatibility. A subcutaneous pocket was created in anesthetized C57BL/6 mice and 200 μL of PEG:dextran was injected into the pocket using a dual chamber syringe equipped with a sterile mixing tip. After nine days, the mice were sacrificed and the skin and subcutaneous tissues were harvested. The samples were snap frozen in liquid nitrogen and stored at −80 °C until histological and zymographic analyses. All experimental protocols were approved by the MIT Animal Care and Use Committee and were in compliance with NIH guidelines for animal use. Harvested tissue was sectioned using cryotome to create 20 μm thick sections. Hematoxylin and eosin staining were performed using standard methods. Fibrotic response was based on morphology and measured in multiple random locations in five images from tissue samples from each mouse. Zymography was performed using quenched fluorescein-labeled gelatin and quantified using Adobe Photoshop as previously published [21].

Adhesive Interface Morphology: To analyze the tissue-specific dependence of PEG:dextran morphology following adhesion, we imaged the tissue-material formed with various soft tissues. Uniform biopsies from freshly harvested rat lung, liver, heart, and duodenum provided a controlled surface area (20 mm^2) for material application. Fluorescently labeled PEG:dextran (50 μL) was applied to tissues after blot drying, and allowed to cure for 30 min. Tissue samples were then cryosectioned (20 μm sections) and stained with rhodamine phalloidin (Invitrogen) and DAPI (Vector Laboratories). PEG:dextran morphology at the tissue-material was quantified using image analysis techniques (Leica Microsystems, MetaMorph®) to characterize the transitory material between tissue surfaces and material bulk.

Aldehyde Affinity of Soft-Tissue Surfaces: To determine the aldehyde affinity of various soft tissues, the conjugation of aldehyde-coated f-MS (Molecular Probes) to soft-tissue surfaces was quantified. Biopsies of rat lung, liver, heart, and duodenum were prepared with equal surface area (20 mm^2) and submerged in 0.5 mL of 0.5% f-MS solutions for 20 min on rocker at 37 °C. Tissue samples were thoroughly rinsed with 10 mL PBS three times. Tissue specimens were then processed and analyzed to quantify the percent surface coverage by f-MS (Leica Microsystems, MetaMorph).

Adhesion Mechanics: The adhesion mechanics following PEG:dextran application to soft tissues was measured with monotonic uniaxial tensile testing (Bose® Biodynamic Test Instrument, Minnetonka, MN, USA). Adhesive test elements were created from a 200 μL application of PEG:dextran evenly distributed between two uniformly sized tissue biopsies (disks of 8 mm diameter, total test element thickness of 1 mm) of rat duodenum, heart, lung, or liver. Tissue surfaces were gently dried prior to material application. After applying PEG:dextran between tissue surfaces and allowing 5 min for material polymerization, adhesive test elements were displaced at a constant rate (0.05 mm s^{-1}) and the load response was continuously recorded (200 measurements s^{-1}). To study the effect of pH on material adhesion strength, tissue samples were submerged in PBS having a pH of 6, 7.3, or 9 for 10 min and left damp for test element construction. Recorded loads were normalized by test element cross-sectional area and reported as an interfacial stress response to a change in thickness.

Material Retention: To track material loss following PEG:dextran adhesion to various soft tissues, fluorescently labeled materials were applied to lung, liver, heart, and duodenum biopsies (4 mm disks). Identical volumes (200 μL) of PEG:dextran (14% dextran aldehyde variant, L-PD) were applied to tissue surfaces and allowed to polymerize for 5 min. Samples were then submerged in PBS at 37 °C for 4 h. The fluorescent signal (485 nm excitation and 538 nm emission) accruing in the media was periodically monitored throughout the suspension period to assess the kinetics of material dissociation from the tissue.

Statistical Analyses: Data are presented as means ± standard deviations. To take multiple comparisons into account, all statistical comparisons were performed using one way ANOVA followed by the Tukey–Kramer test, using InStat software (GraphPad, San Diego, CA, USA). A p-value < 0.05 was considered to denote statistical significance.

Acknowledgements

N.A. and T.S. contributed equally to this work. The authors gratefully acknowledge support from the MIT-DuPont Alliance and National Institutes of Health (R01 GM 49039 to E.R.E) as well as a postdoctoral fellowship from the Philip Morris External Research Program (to A. B. B.).

Received: January 30, 2009
Revised: April 2, 2009
Published online: June 2, 2009

[1] M. Araki, H. Tao, T. Sato, N. Nakajima, H. Sugai, S. H. Hyon, T. Nagayasu, T. Nakamura, *J. Thorac. Cardiovasc. Surg.* **2007**, *134*, 145.
[2] A. Ekelund, O. S. Nilsson, *Int. Orthop.* **1991**, *15*, 331.
[3] C. Vauthier, C. Dubernet, E. Fattal, H. Pinto-Alphandary, P. Couvreur, *Adv. Drug Delivery Rev.* **2003**, *55*, 519.
[4] B. J. Vote, M. J. Elder, *Clin. Experiment. Ophthalmol.* **2000**, *28*, 437.
[5] A. C. van der Ham, W. J. Kort, I. M. Weijma, H. F. van den Ingh, H. Jeekel, *Dis. Colon Rectum* **1992**, *35*, 884.
[6] K. Suzuki, M. Shinya, M. Kitagawa, *J. Obstet. Gynaecol. Res.* **2006**, *32*, 140.

WILEY InterScience® DISCOVER SOMETHING GREAT
© 2009 WILEY-VCH Verlag GmbH & Co. KGaA, Weinheim

[7] K. A. Haukipuro, O. A. Hulkko, M. J. Alavaikko, S. T. Laitinen, *Dis. Colon Rectum* **1988**, *31*, 601.
[8] M. Serra-Mitjans, J. Belda-Sanchis, R. Rami-Porta, *Cochrane Database Syst. Rev.* **2005**, CD003051.
[9] M. Scotte, F. Dujardin, A. Amelot, P. Azema, I. Leblanc, P. Bouvier, F. Michot, P. Teniere, *Eur. Surg. Res.* **1996**, *28*, 436.
[10] R. Rami, M. Mateu, *Cochrane Database Syst. Rev.* **2001**, CD003051.
[11] D. Mutter, M. Aprahamian, C. Damge, P. Sonzini, J. Marescaux, *Biomaterials* **1996**, *17*, 1411.
[12] E. Lim, P. Goldstraw, *Eur. J. Cardiothorac. Surg.* **2007**, *32*, 552.
[13] M. Kawamura, M. Gika, Y. Izumi, H. Horinouchi, N. Shinya, M. Mukai, K. Kobayashi, *Eur. J. Cardiothorac. Surg.* **2005**, *28*, 39.
[14] T. M. Shazly, N. Artzi, F. Boehning, E. R. Edelman, *Biomaterials* **2008**, *29*, 4584.
[15] S. K. Bhatia, S. D. Arthur, H. K. Chenault, G. K. Kodokian, *Biotechnol. Lett.* **2007**, *29*, 1645.
[16] S. K. Bhatia, S. D. Arthur, H. K. Chenault, G. D. Figuly, G. K. Kodokian, *Curr. Eye Res.* **2007**, *32*, 1045.
[17] N. Artzi, T. M. Shazly, C. Crespo, H. K. Chenault, E. R. Edelman, *Macromol. Biosci.* **2009**, DOI: 10.1002/mabi.200800355.
[18] M. B. St Clair, E. Bermudez, E. A. Gross, B. E. Butterworth, L. Recio, *Environ. Mol. Mutagen.* **1991**, *18*, 113.
[19] I. H. de Hingh, H. van Goor, B. M. de Man, R. M. Lomme, R. P. Bleichrodt, T. Hendriks, *Int. J. Colorectal Dis.* **2005**, *20*, 534.
[20] H. G. Yilmaz, M. Odabasi, H. Buyukbayram, B. Bac, *Ulus Travma Derg.* **2001**, *7*, 87.
[21] T. Z. Nursal, R. Anarat, S. Bircan, S. Yildirim, A. Tarim, M. Haberal, *Am. J. Surg.* **2004**, *187*, 28.
[22] M. Gawlak, T. Gorkiewicz, A. Gorlewicz, F. A. Konopacki, L. Kaczmarek, G. M. Wilczynski, *Neuroscience* **2009**, *158*, 167.
[23] J. Clayden, N. Greevs, S. Warren, P. Wothers, *Organic Chemistry*, Oxford University Press, NY **2001**, Ch. 14.

© 2009 WILEY-VCH Verlag GmbH & Co. KGaA, Weinheim